IJCRT.ORG ISSN : 2320-2882

INTERNATIONAL JOURNAL OF CREATIVE RESEARCH THOUGHTS (IJCRT)

An International Open Access, Peer-reviewed, Refereed Journal

Effect of Short-Term Overheating on the Isothermal Oxidation Behavior of P91 Steel

Saraswati Banra[1], Avanish Kumar Chandan[2], A. K. Rajak[3]

[1] Department of Metallurgical Engineering, BIT Sindri, Dhanbad, Jharkhand, India

[2] Materials Engineering Division, CSIR–National Metallurgical Laboratory, Jamshedpur–831007, India

[3] Department of Metallurgical Engineering, BIT Sindri, Dhanbad, Jharkhand, India.

Abstract

P91 ferritic-martensitic steel is widely used in fossil-fires power plants because of its high creep strength and oxidation resistance at elevated temperatures. However, transient overheating above the design temperature can accelerate oxidation, damage the protective oxide scale, and reduce component reliability. In this study, the isothermal oxidation of P91 steel under short-term overheating was investigated in dry air at 600℃ and 800℃ for up to 350 h using weight gain measurements, SEM, cross-sectional analysis, and EDS. The results showed that oxidation increased with both exposure time and temperature, with temperature having the stronger effect. At 600℃, P91 steel formed a thin, compact, and adherent oxide scale with low weight gain. In contrast, at 800℃, the weight gain increased markedly and a much thicker oxide scale developed, with localized cracking and partial delamination. Cross-sectional SEM confirmed faster oxide growth at the higher temperature, while EDS mapping showed a duplex structure with an Fe-rich outer layer and a Cr-rich inner layer. The chromium-rich inner layer was protective at 600℃, but its effectiveness decreased at 800℃ due to rapid oxide growth and enhanced diffusion of oxygen and iron. Overall, short-term overheating significantly reduces the oxidation of P91 steel by accelerating oxide growth and weaking the protective chromium-rich layer. These findings help explain the oxidation behavior of P91 steel during transient overheating in power plant service.

Keywords: High temperature oxidation, isothermal oxidation, short term overheating, oxidation kinetics, oxide spallation, ferritic-martensitic steel.

1. Introduction

During the last fifty years steam pressure and temperature in fossil-fired power plants have been continuously increased to improve thermal efficiency [1]. The thermal efficiency of steam power plant can be significantly improved by increasing the temperature and pressure of the steam entering the turbine inlet from 580 to 620℃ providing a thermal efficiency increase from 38% to 42% [2]. These efficiency gains reduce fuel consumptions as well as CO_2 emissions [2,3]. At such high temperature conventional low-alloy steels and 12% Cr steels can no longer be used as construction materials for live steam piping systems because of the lack of creep resistance of these materials at service temperatures [4].

Consequently, numerous studies on heat resistant steels have been actively conducted since the early 1970s leading to significant progress in both 9-12% Cr steels and austenitic steels [1]. Among these, ferritic-martensitic (F-M) steels are preferred over austenitic stainless steels due to their higher thermal conductivity, lower thermal expansion co-efficient, reduced neutron irradiation-induced swelling, and lower cost [5]. Several modified 9% Cr steels, such as 9Cr-1MoVNb (P91), and 9Cr-2MoVNb (ASME T91), have been developed, in which high-temperature strength is improved through the addition of strong carbide and carbonitride formers elements such as vanadium (V), niobium (Nb) and titanium (Ti) which led to the precipitation of various particles, such as $M_{23}C_6$ and MX type precipitates [1, 6]. Particularly, the modified 9Cr-1Mo (also denoted as ‘‘Grade 91’’) steel is a potential candidate material for power plant industry. P91 grade of steel is used in steam, gas turbine systems and boiler components operating at elevated temperatures in fossil fired thermal and nuclear power plants [6, 7].

For P91 steel oxidation protection is mainly achieved through the formation of protective chromia scale on the alloy surface during high temperature exposure [8]. The approximately 9 wt.% Cr in P91 promotes formation of dense Cr-rich oxides that slow long-term oxidation [5]. Mathiazhagan and Khanna reported that P91 follows parabolic oxidation kinetics in the 600-800°C range, with comparatively lower weight gain and better scale adherence than P92 and E911, consistent with diffusion-controlled oxide growth [9]. Schütze et al. [10] observed stable oxidation of P91 at 650°C in dry synthetic air for exposures up to 10,000 hours with no breakaway oxidation, the stability was attributed to a thin protective chromium oxide and the presence of Mn-rich outer oxides, while Si formed only discrete silica islands at the metal-oxide interface. Long-term service examinations, however, reveal more complex scale structures [10]. Zhong et al. [11] found a two-layer oxide on P91 superheater inner walls where an

outer Fe_2O_3-rich layer lacked detectable Cr and an inner $(Fe, Cr)_3O_4$ layer with a Cr-enriched transition zone; continuous Cr_2O_3 coverage was incomplete, enabling trans granular oxidation. Yonghao et al., [12] compared dry and steam environments and reported that T91 exhibited lower mass gain in dry air (stable up to 600 °C, ~0.6 mg/cm^2 at 700°C) but rough, uneven oxide morphologies and differing resistance in steam vs. dry conditions.

Short-term oxidation studies at the design temperature of 650℃ are limited. Swaminathan et al., [6] reported rapid, non-parabolic oxidation during the first 100 hours, while Schütze et al. [10] observed early formation of a protective chromium-rich scale that may crack after a few hundred hours, indicating that short-term kinetics and scale stability at the design temperature still require further investigation. However, fewer studies have addressed short-term overheating of P91 at temperatures above the design value, despite the fact that transient exposure can expose boiler components to much more severe conditions than normal service [13,14].

In the present study, the isothermal oxidation behavior of P91 steel under short-duration overheating conditions is systematically investigated. The work focuses on understanding the influence of elevated temperature exposure on oxide scale formation, growth kinetics, and spallation behavior. Isothermal oxidation tests conducted at 800°C for different exposure durations are used to simulate overheating conditions experienced by boiler components during transient operation. Special emphasis is placed on evaluating the stability and protectiveness of the Cr_2O_3-rich oxide layer under prolonged high-temperature exposure. The findings are expected to provide deeper insight into the degradation mechanisms of P91 steel and support the safe design and operation of high-temperature steam power plant components.

2. Experimental procedure

Sample specimens were cut from the steel grade namely P91. The chemical composition is tabulated in table-1.

table 1: compositional specification for modified 9cr-1mo steel [14].

Element wt.%	
C	0.08-0.12
Mn	0.30-0.60
P	<0.020
S	<0.010
Si	0.20-0.50
Cr	8.00-9.50
Mo	0.85-1.05
Nb	0.06-0.10
V	0.18-0.25
N	0.03-0.070
Ni	<0.40
Al	<0.04
Fe	Balance

For the oxidation studies the specimens were mechanically polished with SiC papers up to a grit number of 1200 to obtain a smooth and uniform surface finish. The ground specimens were ultrasonically cleaned in acetone to remove surface contaminants and then air dried prior to the oxidation exposure. Microstructures of the modified 9Cr-1Mo steel were revealed by immersion etching in Vilella's reagent (1 g picric acid and 5 ml HCl and 90 ml ethanol).

Each specimen was weighed before oxidation using a digital analytical balance with an accuracy of ±0.0001 g.

High temperature oxidation tests were performed in an electrically heated muffle furnace under an open-air atmosphere. The furnace could operate at temperatures up to 1200°C and was equipped with a PID temperature controller to maintain temperature accuracy within ±2°C.

The prepared specimens were placed in alumina crucibles and positioned in the uniform temperature zone of the furnace. The oxidation experiments were carried out at fixed temperatures of 600°C and 800°C for exposure durations of 50 h, 100 h, and 350 h to investigate the oxidation kinetics.

After completion of the exposure, the furnace was allowed to cool naturally to room temperature.

The oxidized specimens were then carefully removed and re-weighed to determine the weight gain due to oxidation. The weight gain per unit area was calculated and used to evaluate the oxidation behavior of steels.

Hardness tests were conducted on the oxidized specimens.

The oxidized surface and cross sections were examined using an optical microscope and Scanning Electron Microscope coupled with Energy Dispersive X-ray Spectroscopy (SEM/EDS) to characterize morphology and composition.

3. Result and Discussion

The isothermal oxidation behavior of P91 ferritic-martensitic steel was investigated in dry air at 600℃ and 800℃ for exposure durations 50 h, 100 h, 350 h. The oxidation behavior was evaluated from weight gain measurements, surface and cross-sectional scanning electron microscope (SEM), oxide-scale thickness, and energy-dispersive X-ray spectroscopy (EDS). The results demonstrate a pronounced influence of temperature on the oxidation behavior of P91 steel, particularly under the short-term overheating condition of 800℃.

3.1 Oxidation Behavior

table 2: weight gain and percentage weight gain of p91 steel after isothermal oxidation at 600℃ and 800℃.

Temperature (℃)	**Exposure Time (h)**	**Weight Gain (g)**	**Weight Gain (%)**

600	50	0.0100	0.02
600	100	0.0148	0.04
600	350	0.0477	0.11
800	50	0.3436	1.09
800	100	0.7705	2.60
800	350	1.4208	4.35

table 2 summarizes the weight gain and percentage weight gain of p91 steel after oxidation at 600℃ and 800℃. a continuous increase in weight gain with exposure time was observed at both temperatures, confirming progressive oxide formation during isothermal exposure. however, the magnitude of oxidation was strongly dependent on temperature.

At 600℃, the weight gain remained relatively low throughout the exposure period. The weight gain increased from 0.0100 g after 50 h to 0.0477 g after 350 h, while the corresponding percentage weight gain increased from 0.02% to only 0.11%. This relatively small mass increase indicates comparatively slow oxide growth and suggests that the oxide scale formed at 600℃ provided a relatively effective barrier against continued oxidation.

A substantially different behavior was observed at 800. The weight gain increased from 0.3436 g after 50 h to 0.7705 g after 100 h and reached 1.4208 g after 350 h. The corresponding percentage weight gain increased from 1.09% to 4.35%. Thus, increasing the temperature from 600 and 800 resulted in a pronounced increase in oxidation. At 350 h, the percentage weight gain at 800 was approximately higher than that at 600 (4.35% compared with 0.11%)

The strong temperature dependence can be attributed to the increased rates of ionic and oxygen transport through the developing oxide scale at elevated temperature. The higher temperature promotes oxide nucleation and growth and facilitates the transport of iron and oxygen ions through the scale. Under these conditions, the formation and growth of Fe-rich oxides become increasingly significant, while maintaining a continuous and Protective Cr-rich barrier becomes more difficult.

The present weight gain data clearly demonstrates the detrimental effect of overheating at 800 on the oxidation resistance of P91 steel. Although the increase in weight gain with time suggests progressive oxide growth, the available exposure intervals data do not provide sufficient evidence for assigning a specific kinetic law. Therefore, no definite conclusion regarding parabolic, linear oxidation kinetics is made in the present study.

3.2 Surface Morphology of Oxidized Samples

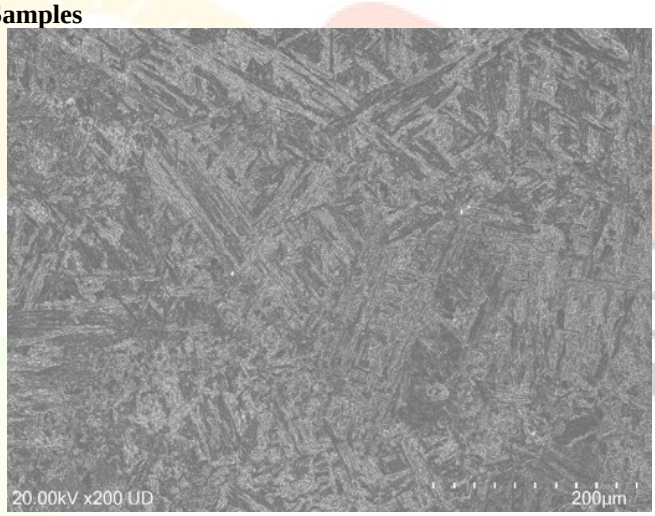

figure 3.1 shows the sem micrograph of the unoxidized p91 sample.

SEM images showed that oxidation temperature strongly affected the oxide morphology. The unoxidized P91 steel had a smooth polished surface, typical of tempered martensitic structure.

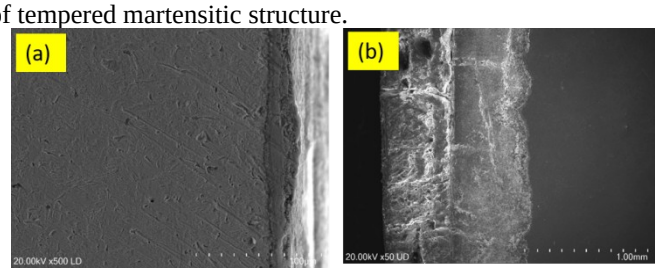

figure 3.2 sem cross-sectional micrographs of p91 steel after isothermal oxidation showing oxide scale development: (a) 600℃-350 h, (b) 800℃-350 h.

SEM image of the oxidized P91 sample showed that the oxide scale changed with temperature. Ater oxidation at 600℃ for 350 h, the oxide layer was thin, compact, and continuous, with very few cracks or sign of peeling. This agrees with the low weight gain observed at 600℃ and indicates that the oxide layer provided good protection against further oxidation. In contrast, the sample exposed at 800℃ for 350 h developed a much thicker and uneven oxide layer. Some cracks and partially detached areas were observed in the oxide layer. These defects may have formed due to the rapid growth of the oxide and the stresses

developed during oxidation. The cracks and detached regions reduced the protective nature of the oxide layer, allowing further oxidation steel.

The difference in the oxide morphology between 600℃ and 800℃ is consistent with weight change measurements. The compact scale at 600℃ corresponds to the relatively low weight gain, whereas the thicker and locally damaged scale at 800℃ corresponds to the substantially higher weight gain. These observations indicate that the protective nature of the oxide scale deteriorates under the overheating condition.

3.3 Oxide Scale Composition and Elemental Distribution

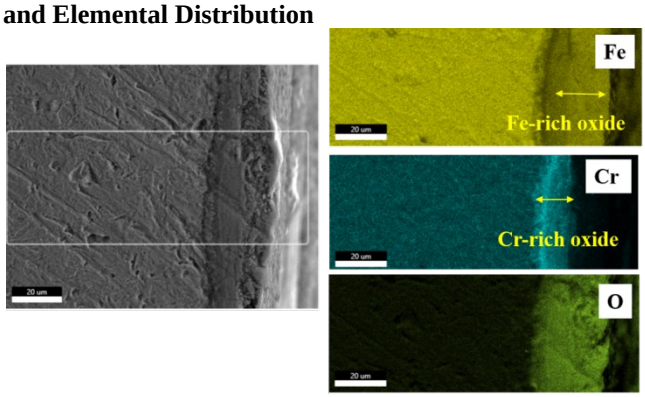

figure 3.3 cross-sectional sem micrograph and corresponding eds elemental maps of fe, cr and o for p91 steel oxidized at 600℃ for 350 h.

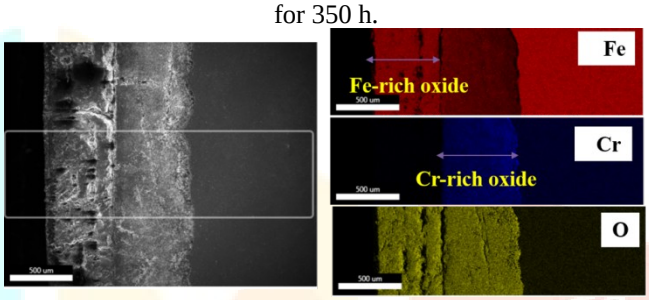

figure 3.4 cross-sectional sem micrograph and corresponding eds elemental maps of fe, cr and o for p91 steel oxidized at 800℃ for 350 h.

The EDS elemental distribution revealed the development of a chemically differentiated oxide scale. An Fe-rich outer region and a Cr-enriched inner region adjacent to the steel substrate were observed at both temperatures. The presence of these regions indicates the selective oxidation and redistribution of alloying elements occur during oxidation.

table 3: thickness of the outer fe-rich oxide layer and inner cr-rich layer formed on p91 steel after 350 h of isothermal oxidation.

Temperature	Outer layer	Thickness (µm)	Inner layer	Thickness (µm)
P91-600℃-350 h	Fe-rich oxide	50	Cr-rich layer	44
P91-800℃-350 h	Fe-rich oxide	90	Cr-rich layer	103

As shown in Table 3, both oxide regions became substantially thicker at 800℃. The thickness of the Fe-rich outer layer increased from approximately 50 µm at 600℃ to 90 µm at 800℃. Similarly, the Cr-rich inner layer increased from approximately 44 µm to 103 µm. The increase in oxide thickness with temperature is consistent with the corresponding increase in weight gain. The formation of a thicker oxide scale at 800℃ indicates enhanced oxidation and increased transport of ions through the growing scale. The substantial development of the Fe-rich outer region is particularly important because Fe-rich oxides generally provide less effective protection than a continuous Cr-rich barrier.

The Cr-enriched inner layer contributes to the oxidation resistance of P91 steel. At 600℃, this layer remained relatively compact and, along with the thin Fe-rich outer layer, provided good protection. At 800℃, the Cr-enriched layer became thicker, but the Fe-rich outer oxide also grew significantly and showed cracks and delamination. Thus, the protective effect of chromium depends on the continuity and stability of the Cr-enriched layer.

3.4 Oxide Growth Mechanism

The combined weight gain, SEM, cross-sectional analysis, and EDS observations provide insight into the oxide growth mechanism of P91 steel. The results are consistent with a diffusion-assisted oxidation process in which oxygen ions and metal ions are transported through the developing oxide scale. The EDS maps indicate the development of an Fe-rich outer region and a Cr-enriched inner region, suggesting that different species participate in oxide growth at different locations within the scale.

At 600℃, oxidation proceeds relatively slowly, as indicated by the very small mass increase and limited oxide thickness. The C-enriched inner regions remain comparatively compact and, together with the outer oxide, provides a relatively effective barrier to further transport. Consequently, the oxide scale remains adherent and the overall oxidation rate remains low.

At 800℃, the substantially higher temperature accelerates the processes responsible for oxide formation and growth. The resulting scale contains a significantly thicker Fe-rich outer layer region and Cr-enriched inner region. The rapid development of the oxide scale can generate thermal stresses, which contribute to localized cracking and partial delamination. Once these defects

develop, the protective effectiveness of the scale is reduced, facilitating continued oxidation and contributing to the substantially higher weight gain observed at 800℃.

The proposed oxide-growth sequence is therefore characterized by the initial development of a Cr-enriched region near the metal/oxide interface followed by substantial growth of Fe-rich oxide toward the outer surface. At the normal service related-temperature investigated here 600℃, the resulting scale remains comparatively thin and compact. Under the short-term overheating condition 800℃, accelerated oxide growth and scale damage become dominant features, resulting in reduced oxidation resistance

Overall, the results demonstrate that the oxidation resistance of P91 steel is strongly associated with the integrity of the Cr-enriched inner region and the ability of the oxide scale to remain continuous and adherent. The degradation of this protective configuration of 800℃ explains the substantially greater weight gain and oxide scale development observed under the overheating condition.

Acknowledgement

The authors gratefully acknowledge the support and facilities provided by the CSIR–National Metallurgical Laboratory (NML), Jamshedpur, for carrying out the experimental work. The authors also sincerely acknowledge the guidance and support received from the faculty and staff of the Department of Metallurgical Engineering, BIT Sindri, Dhanbad, during the course of this work.

4. Conclusion

1. Oxidation increased with both exposure time and temperature; however, temperature produced the most pronounced effect.

2. P91 exhibited comparatively good oxidation resistance at 600℃. The low weight gain increased and relatively compact oxide morphology indicate the development of a comparatively protective and adherent oxide scale.

3. Overheating at 800℃ substantially accelerated oxidation.

4. The oxide scale exhibited a chemically distinct structure consisting of an Fe-rich outer region and a Cr-enriched inner region.

4. The Cr-enriched inner region played an important role in maintaining oxidation resistance.

References

1. Fujimitsu Masuyama, "History of Power Plants and Progress in Heat Resistant Steels," ISIJ International, vol. 41, no. 6, pp. 612-625, 2001.

2. Ehlers, J., Young, D. J., Smaardijk, E. J., Tyagi, A. K., Penkalla, H. J., Singheiser, L., & Quadakkers, W. J. (2006). Enhanced oxidation of the 9%Cr steel P91 in water vapor containing environments. Corrosion Science, 48(12), 3428-3454.

3. Hagarová, M., Baranová, G., Fujda, M., Matvija, M., Horňak, P., Bednarčík, J., & Yudina, D. (2022). High temperature oxidation behavior of creep resistant steels in water vapour containing environments. Materials, 15(2), 616. https://doi.org/10.3390/ma15020616

4. Maruyama, K., Sawada, K., & Koike, J. (2001). Strengthening mechanisms of creep resistant tempered martensitic steel. ISIJ International, 41(6), 641-653.

5. Rai, A. K., Biswal, R., Gupta, R. K., Rai, S. K., Singh, R., Goutam, U. K., Ranganathan, K., Ganesh, P., Kaul, R., & Bindra, K. S. (2019). Enhancement of oxidation resistance of modified P91 grade ferritic-martensitic steel by surface modification using laser shock peening. Surface and Coatings Technology.

6. Swaminathan, S., Mallika, C., Krishna, N. G., Thinaharan, C., Jayakumar, T., & Kamachi Mudali, U. (2014). Evolution of surface chemistry and morphology of oxide scale formed during initial stage oxidation of modified 9Cr-1Mo steel. Corrosion Science, 79, 59-68. DOI.org/10.1016/j.corsci.2013.10.026

7. Krishna Guguloth, & Nilima Roy. (2017). Creep deformation behavior of 9Cr1MoVNb (ASME Grade 91) steel. Materials Science and Engineering: A, 680, 373–381. https://doi.org/10.1016/j.msea.2016.10.112

8. L. Liu, Z.-G. Yang, C. Zhang, M. Ueda, K. Kawamura, & T. Maruyama. (2012). Effect of water vapor on the oxidation of Fe–13Cr–5Ni martensitic alloy at 973 K. Corrosion Science, 63, 1–9.

9. P. Mathiazhagan and A. S. Khanna, "High temperature oxidation behavior of P91, P92 and E911 alloy steels in dry and wet atmospheres," High Temperature Materials and Processes, vol. 30, no. 1-2, pp. 43-50, 2011. Doi.org/10.1515/HTMP.2011.006

10. M. Schütze, M. Schorr, D. P. Renusch, A. Donchev, & J. P. T. Vossen (2004). The role of alloy composition, environment and stresses for the oxidation resistance of modern 9% Cr steels for fossil power stations. Materials Research, 7(1), 111–123.

11. Wanli Zhong, Zhenggang Li, Wei Wang, & Bing Yang. (2012). Research on the microstructure and the growth mechanism of oxidation film of T91 steels after service. Advanced Materials Research, 476–478, 144–150. DOI.org/10.4028/www.scientific.net/AMR.476-478.144

12. Leong, Y., Alia, F., & Kurniawan, T. (2016). High temperature oxidation behavior of T91 steel in dry and humid condition. Indonesian Journal of Science and Technology, 1(2), 232–237.

13. Burja, J., Batič, B. Š., Žužek, B., & Balaško, T. (2023). High-temperature oxidation of boiler steels at 650 °C.

14. King, J. F., Sikka, V. K., Santella, M. L., Turner, J. F., & Pickering, E. W. (1986). Weldability of modified 9Cr-1Mo steel. Oak Ridge National Laboratory.

IJCRT